Scilight

Innovations in Space Research Technology
https://www.sciltp.com/journals/SpaceTech

Review

Cosmic Ray Space Experiments †

Martin Pohl

Department of Nuclear and Particle Physics (DPNC), University of Geneva, 1211 Genève, Switzerland; martin.pohl@unige.ch
† This review draws on an article written for the forthcoming Elsevier Encyclopedia of Particle Physics by the same author.

How To Cite: Pohl, M. Cosmic Ray Space Experiments. *Innovations in Space Research Technology* **2026**, *1*(1), 1.

Received: 24 September 2025
Revised: 25 October 2025
Accepted: 5 November 2025
Published: 4 December 2025

Abstract: This article describes current experiments in space which measure charged cosmic ray particles in the range from 10 GV to 10^5 GV of magnetic rigidity $p/(Ze)$. In this energy range, cosmic rays are expected to originate from sources in the Milky Way and be confined to our galaxy. Technologies and methods to study the spectra of electrons, positrons and nuclei are described, as well as the analysis of antimatter components. Figures of merit for instruments currently in orbit are discussed.

Keywords: cosmic rays; space experiments; PAMELA; AMS-02; CALET; DAMPE; HERD

1. Introduction

The exploration of primary cosmic radiation in Low Earth Orbit started together with the space age itself. Pioneering measurements were made by James A. Van Allen in 1947 [1] using a V2 rocket, spoils of World War II recuperated from Germany together with its inventor Wernher von Braun. The rate of a single Geiger-Müller counter installed at the tip of the ballistic rocket is shown in Figure 1. It shows how the count rate falls beyond the Regener-Pfotzer maximum to reach a plateau above about 60 km altitude. Although these data are not corrected for back-splash from the atmosphere, this is arguably the first time that the direct observation of genuine primary cosmic rays has been reported.

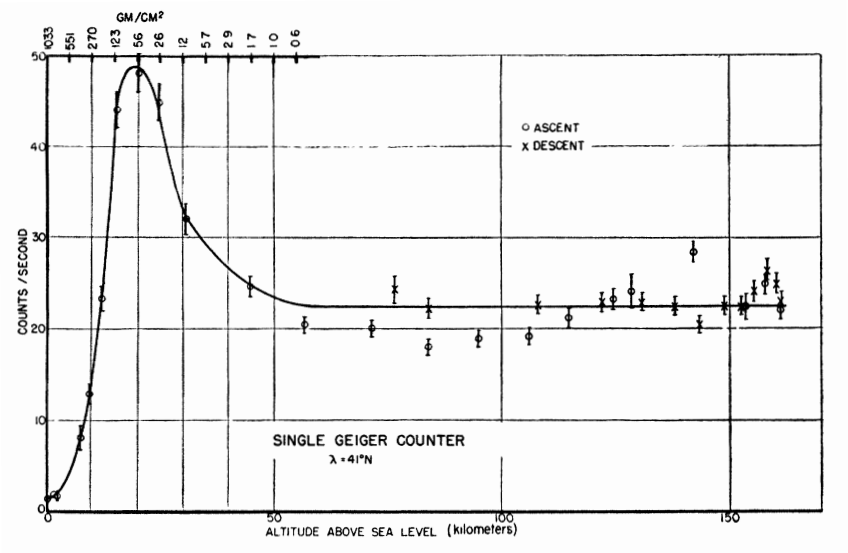

Figure 1. Count rate of a single unshielded Geiger-Müller counter installed at the tip of a V2 ballistic rocket as a function of altitude above sea level (Figure 4 in Ref. [1]).

In the 1960s and 1970s, the Soviet Union PROTON and SOKOL satellite detectors made first attempts of calorimetric energy measurements combined with rudimentary particle identifications [2–6]. The devices used in the PROTON space flights were sampling calorimeters of gradually increasing thickness preceded by a carbon target [7].

The particle identification by proportional chambers and a Cherenkov counter was compromised by back-splash from the carbon target. However, the energy measurements stay a reference for low-energy all-particle spectra [6]. The SOKOL mission also used a sampling calorimeter with scintillators as active elements, but preceded it by a dual set of Cherenkov counters to fight backsplash [8]. The NUCLEON detector [9], in orbit from 2014 to 2017, was a modern implementation of this basic design.

The pioneer of cosmic rays spectrometers in space was the PAMELA detector, launched in 2006 as an attached payload on a Russian Earth observation satellite [10], with the specific task of studying cosmic antimatter. A sketch of the set-up is shown in Figure 2. Its heart was a small magnetic spectrometer of $13 \times 16\,\mathrm{cm}^2$ active surface inside a permanent magnet providing a uniform field of $\sim 0.48\,\mathrm{T}$. Ferromagnetic shielding outside the magnet reduced field leakage. Six layers of double-sided silicon micro-strip detectors tracked particles with high precision and measured their specific energy loss $\mathrm{d}E/\mathrm{d}x \propto Z^2$, for a total geometrical acceptance of $21.5\,\mathrm{cm}^2\mathrm{sr}$. The spectrometer thus reached a maximum detectable magnetic rigidity (MDR) (The magnetic rigidity of a particle is the momentum per unit of charge, $p/(Ze)$. Particles with the same rigidity follow the same trajectory in a magnetic field. The maximum detectable rigidity (MDR) of a spectrometer is defined as the magnetic rigidity where the relative measurement error reaches 100%.) of the order of $1\,\mathrm{TV}$ [11]. The set-up was completed by scintillation detectors and an electromagnetic calorimeter, with tail catcher and neutron detector to help distinguish hadronic showers. PAMELA's orbit was first a quasi-polar (70°) elliptical one at altitudes between 355 and $584\,\mathrm{km}$, changed in 2010 to a circular orbit at $550\,\mathrm{km}$. The duration of the mission, originally planned to be three years, turned out to be about ten years, during which the efficiency of the device changed from about 90% in 2006 to 20% after 2014, due to radiation damage to the tracking detector front-end chips [12]. A rich physics output resulted from the mission [12]. In particular, results for the positron spectrum showed for the first time an excess with respect to pure secondary production [13,14].

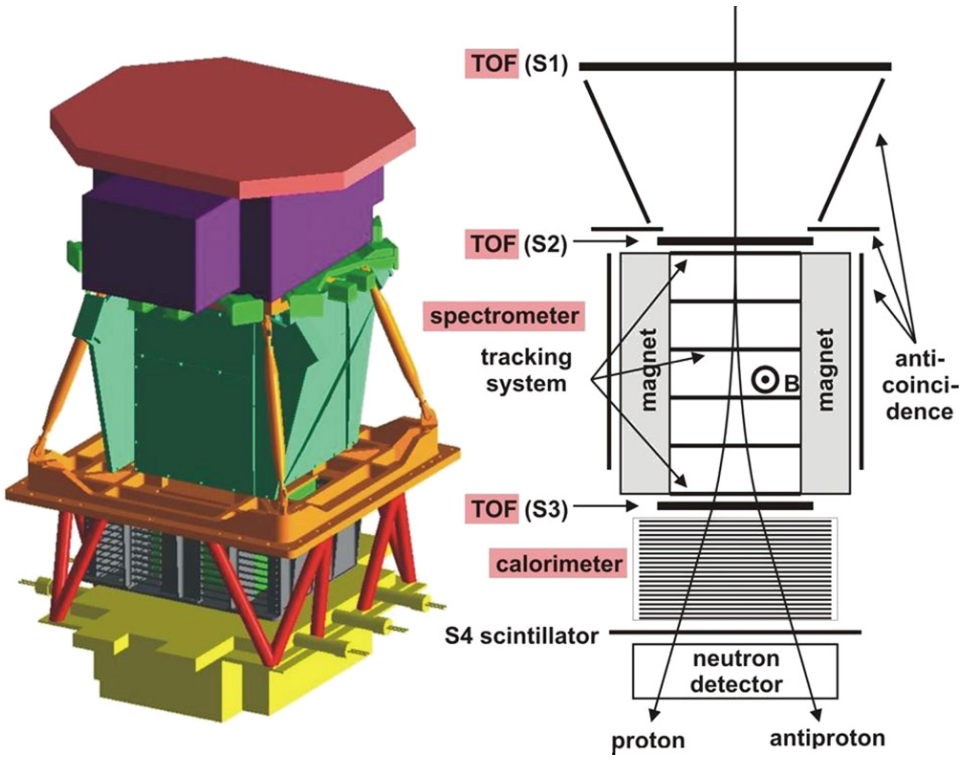

Figure 2. Schematic of the PAMELA satellite spectrometer and its components [15]. A time-of-flight (TOF) system with three layers determines the particle flight direction and triggers the data taking. A spectrometer with a permanent magnet and six layers of solid state tracking detectors measures the magnetic rigidity. A calorimeter with tail catcher and neutron detector completes the set-up.

With the PAMELA project, not only modern particle detection technology but also strict analysis techniques migrated from accelerator experiments into space. Previous experiments had often suffered from little control of experimental systematics, as can be concluded from the large spread of measured flux values reported by different experiments even for the most abundant cosmic ray species [16]. This dramatically changed with the PAMELA mission. Sophisticated and redundant hardware, large acceptance and thorough calibration in accelerator particle

beams yield better controlled systematics, together with excellent statistical accuracy of the data. The next such detector was the Alpha Magnetic Spectrometer, built by a collaboration of accelerator particle physicists led by Samuel C.C. Ting of MIT. NASA required the collaboration to first build a demonstrator prototype, called AMS-01, to travel on the Space Shuttle. The detector had about one half of the spectrometer equipped inside a permanent magnet. Simplified particle identification equipment surrounded the spectrometer.

The prototype detector flew on Space Shuttle Discovery's flight STS-91 in June 1998, the last Space Shuttle mission to the Russian Mir station. It successfully collected 70 million cosmic rays in ten days. Details of the set-up, performance and physics result are summarised in a comprehensive report [17]. Based on the success of this precursor, a more ambitious detector, AMS-02 discussed in Section 2.1, was constructed for a long-term installation on the ISS, and installed in 2011. Since 2015, large-size calorimeters are also in operation, such as DAMPE on a free-flying Chinese satellite, and CALET on the ISS; these are discussed in Section 2.2.

2. Cosmic Ray Detectors in Space

Space experiments are a privileged way of pursuing research on cosmic ray since they allow to study them *in situ* before they interact in the Earth's atmosphere. The ISS provides an ideal platform for the long-term exposure of sophisticated particle detectors. The year 2020 marked the twentieth anniversary of constant manning for the ISS, 2021 the tenth year of data taking by the Alpha Magnetic Spectrometer. New cosmic ray calorimeters have been deployed in the meantime.

The power law shape of the cosmic ray all-particle spectrum has driven a two-fold experimental approach to the detection of cosmic rays. Space-borne and balloon detectors are employed to measure cosmic ray spectra and elemental composition at energies approaching 10^6 GeV. Above this energy, the particle flux summed over a whole hemisphere is less than a few particles per square meter per year and rapidly decreases to about 100 particles per square kilometre per year at 10^9 GeV, thus requiring kilometre-size observatories which can only be deployed on the Earth's surface. Space-born detectors have direct access to cosmic ray particles before they enter the Earth's atmosphere and cause air showers. The accurate identification of the incoming cosmic ray particle is thus experimentally feasible.

Both spectrometry-based and calorimetry-based cosmic ray observatories are currently active in space missions. The primary observable of spectrometers is the magnetic rigidity, i.e. the signed ratio of particle momentum and electric charge. For all astrophysical processes involving magnetic fields, like in acceleration and transport of cosmic rays, rigidity is indeed the relevant quantity. Spectrometers are generally equipped with additional detectors for particle identification, to enhance their capability to assess particle charge and distinguish light from heavy particles. Cosmic ray antiparticles can only be distinguished from particles by direct detection with a magnetic spectrometer, since there is no way to measure the sign of the electric charge by calorimetric means. Pioneers in the direct measurement of the spectra for individual cosmic ray species have been the balloon-borne magnetic spectrometer BESS [18,19] and the satellite experiment PAMELA shown in Figure 2.

Magnetic spectrometers equipped with velocity measuring devices also have the ability of measuring the isotopic composition of light nuclei. However, with current state-of-the-art technology, isotopic composition can be measured only at energies below about $10\,\mathrm{GeV/n}$. Thus nuclei spectra are usually summed over isotopes.

Calorimetric detectors, on the other hand, are more compact and can thus cover a large solid angle. Current experiments can thus make meaningful flux measurements up to PeV energies, but do not distinguish between particles and antiparticles. Calorimeters are robust and can take data unattended over long periods of time. Their primary observable is the kinetic energy of the incident particle. The energy resolution of a calorimeter generally improves with energy until reaching a plateau, while the resolution of magnetic spectrometers worsens with rigidity. When combined with devices for the measurement of particle charge, calorimeters deliver the energy spectrum of individual cosmic ray species, summing over particles and antiparticles as well as isotopes.

Spectra are thus measured as a function of magnetic rigidity by spectrometers, as a function of kinetic energy by calorimeters. Conversion from one quantity to the other requires an assumption about the isotopic composition of the observed elements based on available measurements or theory.

2.1. The Alpha Magnetic Spectrometer AMS-02

The only magnetic spectrometer currently acquiring cosmic ray data is the **Alpha Magnetic Spectrometer (AMS-02)** shown in Figure 3. AMS-02 was installed on the ISS in May 2011 and has been taking data since. In its first 10 years of operation it has collected and analysed over 180 billion cosmic rays. We briefly describe its principle components and their performance; more details are available in Reference [20]. The AMS-02 components, shown in Figure 4, have been designed to perform simultaneous and accurate measurements of the individual spectra of

positrons, electrons, antiprotons, protons and nuclei up to the nickel region ($Z \sim 30$). The spectrometer has a reach in magnetic rigidity from a fraction of a GV up to a few TV.

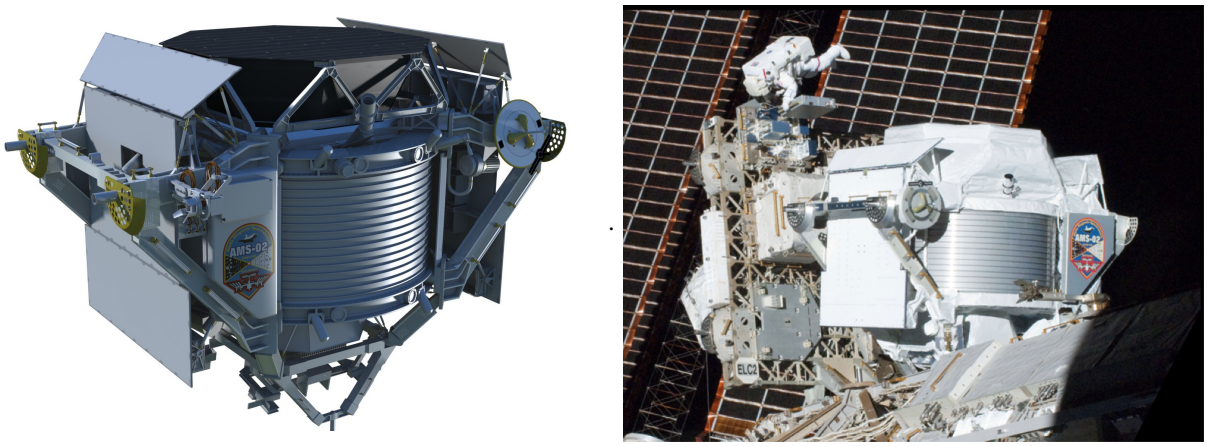

Figure 3. Left: Artists impression of the AMS-02 detector (Credit: NASA). **Right**: The AMS-02 instrument installed on the main truss of the ISS with an astronaut working in a nearby site (Credit: NASA).

Particles enter the detector from the top, in the negative z-direction in the coordinate system indicated in Figure 4. The heart of the detector is a spectrometer comprising a cylindrical permanent magnet and silicon sensors tracking the particle trajectory. The dipolar field is generated by 64 NdFeB blocks arranged in a Halbach array, reaching $0.15\,\mathrm{T}$ in the centre. It points in the x-direction, bending the trajectory in y. The trajectory is located by nine layers of silicon strip detectors. The tracking layers are arranged with six layers inside the magnet bore and three outside. The rigidity measurement thus results from a mixture of sagitta and bend-angle measurements. The relative rigidity resolution is about $\Delta R/R \simeq 0.1$ for $R < 20\,\mathrm{GV}$ and increases with rigidity. The maximum detectable rigidity varies between $2.0\,\mathrm{TV}$ for protons and $3.7\,\mathrm{TV}$ for iron nuclei. The spectrometer is completed by a large set of partially redundant devices identifying particles and measuring their kinetic energy, as described in Figure 4. AMS-02 is installed on the ISS since May 2011. Until the end of September 2025, it has collected over 255 billion cosmic ray particles (The current count rate is constantly updated at https://ams02.space (accessed on 24 September 2025), arguably the largest sample since the discovery of cosmic rays. The collaboration plans to continue operating the observatory until the end of the ISS lifetime.

The AMS-02 detector components are listed in Figure 4. We describe the components in the order in which they are encountered:

- The **Transition Radiation Detector** (TRD) has twenty layers. Each layer is composed of a $20\,\mathrm{mm}$ thick fleece radiator and a layer of proportional tubes for X-ray detection. The TRD distinguishes light from heavy particles, by measuring the transition radiation emitted at highly relativistic velocities. It identifies one positron in a background of more than 1000 protons at 90% positron detection efficiency.
- The **Time-Of-Flight** system (TOF) consists of two double layers of scintillation detectors placed above and below the magnet, covering about $1.6\,\mathrm{m}^2$ each. They measures the time a particle takes to traverse from the top to the bottom layer with a resolution ranging from $160\,\mathrm{ps}$ for singly charged ($Z = 1$) particles down to $50\,\mathrm{ps}$ for heavier ($Z > 6$) nuclei. The TOF measures the cosmic ray arrival direction and velocity, and gives the **trigger** for charged particles to the overall data acquisition system.
- Sixteen **Anticoincidence Counters** (ICC) surround the inner bore of the magnet to reject particles entering the detector from the sides with an efficiency of 0.99999.
- The heart of the detector is a **magnetic spectrometer** composed of a cylindrical permanent magnet, and a tracker. The magnet generates a dipolar field with the main component directed along the x-axis. The tracker has nine layers of double-sided silicon micro-strip detectors. Layers L3 to L8 are inside the magnet bore, L2 above the magnet, L1 on top of the TRD and L9 just above the electromagnetic calorimeter (ECAL). The total lever arm from L1 to L9 is $3\,\mathrm{m}$. At each tracker layer the x- and y- coordinates of the particle impact point are measured with accuracies of 13 to $20\,\mu\mathrm{m}$ and 5 to $10\,\mu\mathrm{m}$ respectively. The bending of the particle trajectory inside the magnetic field gives the rigidity, $R = p/(Ze)$, and its direction allows to distinguish positively charged particles from negatively charged particles.
- The **Ring Imaging Cherenkov counter** (RICH) is composed of a radiator plane made of NaF and silica aerogel, a conical mirror on the sides, and a photon-detection plane at the bottom. The particle's velocity is obtained from the aperture angle of the Cherenkov light cone with a relative resolution better than 0.1%,

allowing to measure isotopic composition of light nuclei up to $\sim 10\,\mathrm{GeV/n}$. The **particle charge** squared, Z^2, is measured independently from the intensity of the emitted light in the RICH, and from the energy deposited in the active detector materials of TRD, TOF, Tracker and ECAL.

- The 3D sampling **Electromagnetic Calorimeter** (ECAL) is made of nine multi-layered lead and scintillating fibre sandwiches for a total of 17 X_0. The nine sandwiches are stacked such that the fibres run alternatively along the x-coordinate (five layers) and the y-coordinate (four layers). ECAL measures the energy of electrons and positrons with few percent accuracy. It also gives the **trigger** to the overall data acquisition for photons and measures their energy. The 3D reconstruction of the particle shower in ECAL, and the matching of the energy measured in ECAL with the momentum measured in the tracker give an additional discrimination power to separate leptons ($\mathrm{e}^{\pm}$) from hadrons (p and $\bar{\mathrm{p}}$) better than 1 positron over 10,000 protons at 90% positron detection efficiency, independent of the TRD. The ECAL also allows to calibrate the rigidity scale of the spectrometer *in situ* using cosmic rays electrons and positrons.

The complete detector in its flight configuration has been carefully calibrated in particle beams at CERN just before launch. Calibration and alignment of components are constantly updated and refined during data taking on the ISS (Section 1 in Ref. [20]).

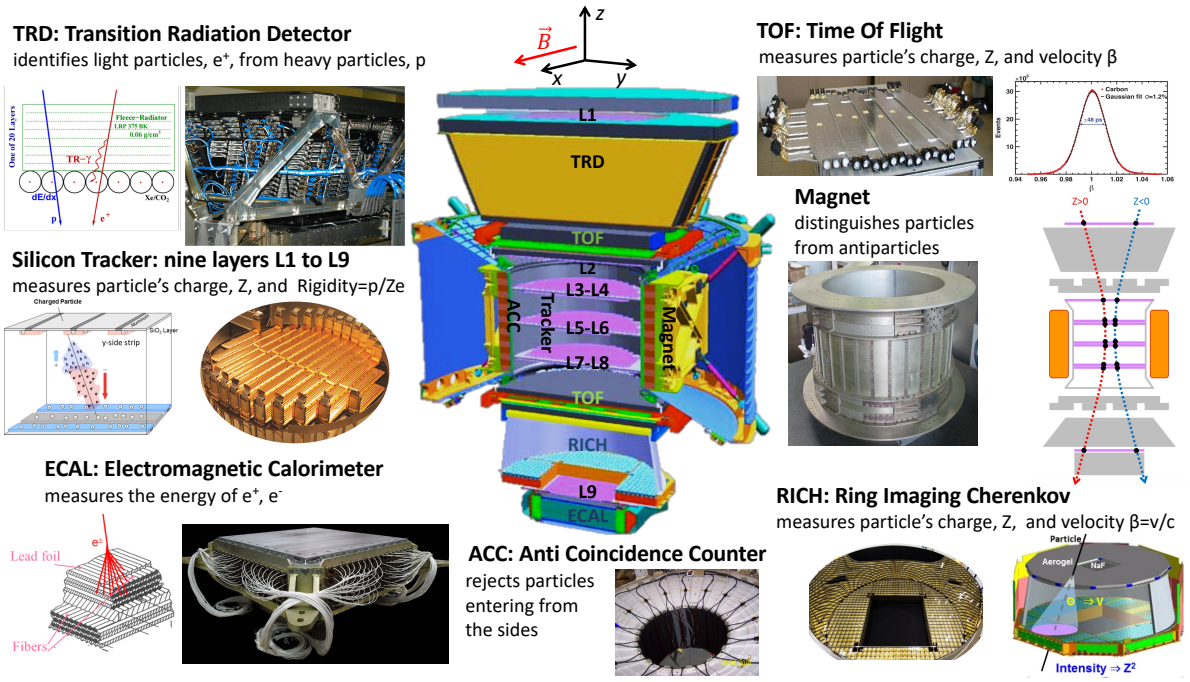

Figure 4. Schematic cut through the AMS-02 detector (centre) showing its components, TRD, TOF, Tracker, Magnet, ECAL, ACC, and RICH, with their main functions (adapted from [20]). Cosmic rays are detected entering the instrument from the top.

2.2. The Calorimetric Cosmic Ray Detectors CALET and DAMPE

Since 2015, the energy region beyond a few TeV is being explored with large-size calorimeters, such as DAMPE [21] on a free-flying Chinese satellite, and CALET [22] on the ISS. This pushes the frontier of current direct cosmic ray measurements to 10^6 GeV and potentially towards knee energies as more data are collected. The DAMPE and CALET missions both started in 2015 and are currently operational. They have collected several billion cosmic rays until the end of 2023.

The **Calorimetric Electron Telescope (CALET)** has been developed to measure the cosmic ray $\mathrm{e}^{\pm}$ spectrum in the kinetic energy range from 1 GeV to 20 TeV, the gamma-ray spectrum up to 10 TeV and the proton spectrum from 50 GeV to 1000 TeV. The individual spectra of nuclei can be measured in the kinetic energy range from 10 GeV to 1000 TeV, for nuclei up to iron as well as trans-iron nuclei up to $Z \sim 40$ [22]. CALET has been launched by a Japanese mission to the ISS and takes data since October 2015. The CALET set-up and its position on the ISS are shown in Figure 5. Cosmic rays entering from the top are measured in the following three detectors:

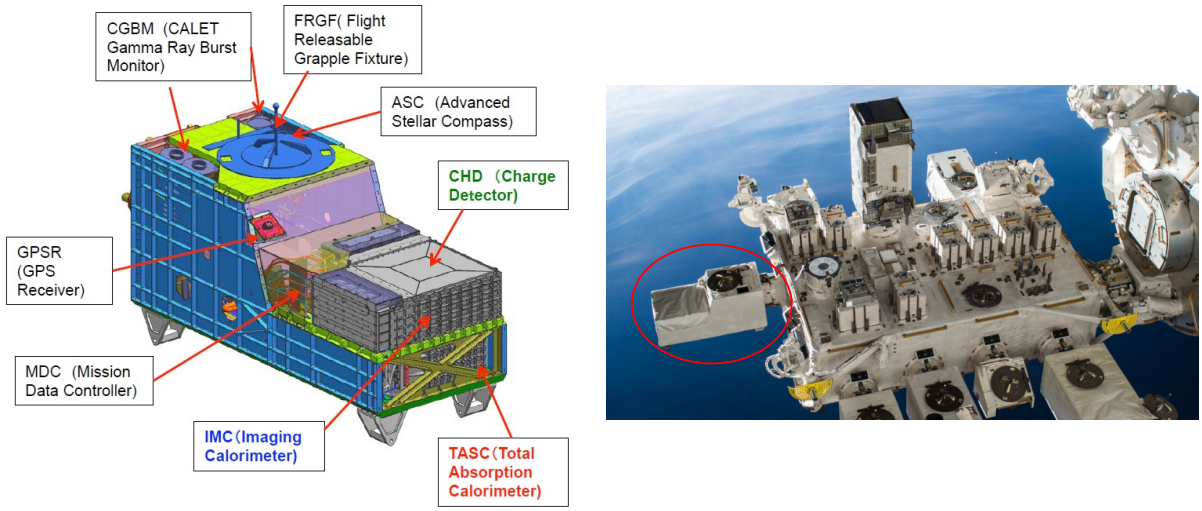

Figure 5. Left: Principle components of the CALET calorimetric detector [23] with the charge measurement device (CHD) followed by an imaging calorimeter (IMC) and a total absorption calorimeter (TASC) for electromagnetic showers. The CALET payload is also equipped with a gamma-ray burst monitor (CGBM). **Right**: The CALET instrument (ellipse) installed on the Exposed Facility of the Japanese Experiment Module on the ISS (Credit: JAXA/NASA).

- The **Charge Detector** (CHD) is made of a double layer of scintillators read by photomultiplier tubes (PMT). The signal of each CHD layer is used as input to trigger the overall data acquisition. The CHD measures the absolute value of the particle charge from the energy deposited in the scintillator. Its large dynamic range allows to identify nuclei up to $|Z| \sim 40$.
- The **Imaging Calorimeter** (IMC) is a 3D sampling calorimeter with a total depth equivalent to $3\,X_0$, covering a surface of $45 \times 45\,\mathrm{cm}^2$. It is made of seven layers of tungsten alternated with two layers of scintillating fibres (SciFi) arranged orthogonally, and capped by additional SciFi double layers for a total of 16 active layers. The fibres are read individually by multi-anode photomultiplier tubes (MAPMT). The IMC provides a 3D reconstruction of the early phase of the incoming particle shower allowing to determine the shower starting point and the cosmic ray arrival direction with angular resolutions of $0.14°$ for electrons and $0.24°$ for photons. The IMC also measures the absolute value of the charge for nuclei up to silicon ($Z = 14$) from the energy deposited in the SciFi fibres. For each IMC double layer the signals from the two SciFi layers are combined to generate input to the trigger system.
- The **Total Absorption Calorimeter** (TASC) is a homogenous calorimeter equivalent to $27\,X_0$. It consists of twelve layers of lead tungstate (PWO), each composed of 16 PWO logs. The layers are arranged alternating between logs in orthogonal directions to allow 3D reconstruction of the particle shower. The PWO logs of the first layer are read individually by a photomultiplier tube (PMT) to provide additional input to the trigger system. The remaining eleven layers are read by silicon photodiodes and avalanche photodiodes (Dual PD/APD). The read-out system is configured to provide sufficient dynamic range to measure energy depositions from MIP to showers induced by a $1\,\mathrm{PeV}$ proton.The TASC measures the energy of electrons with a resolution better than 2% above $20\,\mathrm{GeV}$. IMC and TASC together represent a thickness of $\sim 1.3\lambda_I$ for hadrons.
- The **trigger** for the data acquisition is obtained combining the signals from the CHD layers, the IMC layers, and the first TASC layer [24]. Leptons ($\mathrm{e}^{\pm}$) are distinguished from protons and nuclei by comparing the 3D reconstruction of their shower in the IMC and TASC. The discrimination power is of the order of 1 electron over a background of 10^5 protons with less than 10% proton contamination up to $7.5\,\mathrm{TeV}$ [25], using an innovative boosted decision tree analysis.

CALET components have been calibrated before launch in particle beams at CERN, the calibration is constantly updated using flight data [24]. Until the end of 2023, CALET has registered about 2 billion cosmic rays with an energy exceeding $10\,\mathrm{GeV}$.

Based on the successful balloon detectors CREAM, an evolved version ISS-CREAM [26,27] was installed on the ISS in 2017 on the same platform as CALET. The detector components are similar to the balloon version. It took data for 18 months from August 2017 to February 2019, before it was stopped prematurely by NASA management, after an estimated life-time of only 228 days [28].

The **Dark Matter Particle Explorer (DAMPE)** measures the spectra of photons and $\mathrm{e}^{\pm}$ in the energy range

5 GeV to 20 TeV, and the spectra of protons and nuclei up to iron ($Z \leq 26$) in the kinetic energy range from 50 GeV to 1 PeV. The DAMPE satellite was launched in December 2015 on a Chinese carrier. It follows a sun-synchronous orbit of about 500 km radius. The principle components of the detector are shown in Figure 6:

- The **Plastic Scintillator Detector** (PSD) measures the charge of incident particles and provides charged-particle background rejection for gamma rays. The PSD has an active area of $82.5 \times 82.5\,\mathrm{cm}^2$. It consists of 82 plastic scintillator bars arranged in two orthogonal planes, each equipped with a double layer. Each bar is read out at both ends with a wide dynamic range extending up to 1400 times the energy deposition of a minimum ionising particle (MIP), so that it can identify nuclei up to $Z \simeq 40$ [29].
- The role of the **Silicon-Tungsten Tracker Converter** (STK) is to provide precise particle track reconstruction, measure the electrical charge of incoming cosmic rays and convert incoming photons to electron-positron pairs. It consists of six orthogonally oriented double planes of position-sensitive silicon detectors with a total area of about $7\,\mathrm{m}^2$, with a single hit resolution of about 50 µm. Multiple thin tungsten layers enhance the photon conversion rate while keeping multiple scattering of electron-positron pairs at a negligible level for energies above 50 GeV. The total thickness of STK is about $1\,X_0$.
- The **BGO calorimeter** (BGO) measures the energy deposition of incident particles. It images the 3D profile (both longitudinal and transverse) of the shower development, and thus provides electron/hadron discrimination. And it provides the main trigger for the DAMPE data acquisition. It consists of bismuth germanate (BGO) bars, arranged in 14 layers with alternating orthogonal durections, comprising 22 bars each. Its total area coverage is $60 \times 60\,\mathrm{cm}^2$, the total depth amounts to $32\,X_0$ at normal incidence. For electromagnetic showers, it has the percent-level energy resolution typical for this material. For hadronic showers, the resolution is about 30% [30].
- The **Neutron Detector** (NUD) acts as a tail catcher for hadronic showers. Its blocks of boron-loaded plastic scintillator are sensitive to neutron capture signalled with a fixed delay of $2\,\mu$s with respect to the trigger. The NUD thus contributes to the distinction between hadronic and electromagnetic showers. It enhances the rejection of hadronic showers by more than a factor of ten.

Components have been calibrated before launch in particle beams at CERN, the calibration is constantly updated using flight data. Until the end of 2023, DAMPE has registered about 15 billion cosmic rays and photons with an energy exceeding 20 GeV.

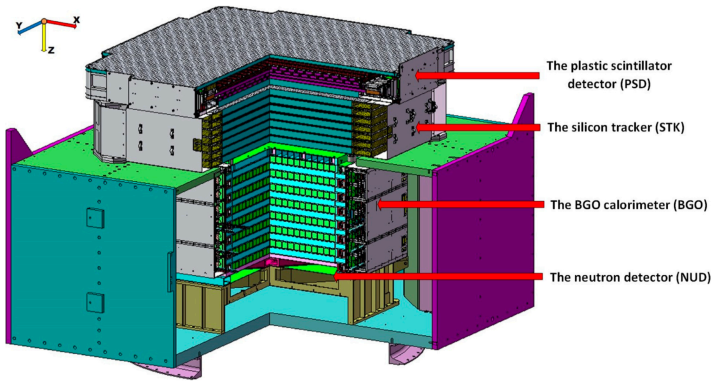

Figure 6. Principle components of the DAMPE [21] free-flying calorimetric cosmic ray detector, composed of a Plastic Scintillator Detector (PSD) and a Silicon-Tungsten tracker-converter (STK) for charge measurement, a BGO imaging calorimeter of $32\,X_0$ depth for energy measurement, and a Neutron Detector (NUD), which together with the calorimeter provides lepton/hadron identification.

3. From Data to Physics

Cosmic ray experiments identify and count cosmic ray particles as a function of particle type, magnetic rigidity or energy, direction and time of arrival. These observables are used to measure the differential cosmic ray flux, for single species, groups of particles or all particles.

The differential flux $\mathrm{d}\Phi/\mathrm{d}E$ is given by the number of particles $\Delta N(E)$ counted in a time window Δt and an energy window between E and $E + \Delta E$. The integral flux $\Phi(E)$ is obtained integrating the differential flux above a threshold energy E. When the flux is measured by a detector covering an acceptance A, defined by its active

surface, solid angle coverage and total detection efficiency, it is given by:

$$\frac{\mathrm{d}\Phi(E)}{\mathrm{d}E} = \frac{\Delta N(E) - B}{A\,\Delta t\,\Delta E} \tag{1}$$

The raw number of particle counts ΔN needs to be corrected for the background counts B. The acceptance A of a detector includes three main factors:

- A geometrical factor G ($[G] = [\mathrm{m^2 sr}]$) defined by the active surface and solid angle coverage. It may depend on particle type, since different sub-systems may be required for their identification.
- The efficiency ϵ_T to trigger the data acquisition when a particle of the given species passes through G.
- The efficiency ϵ_S of the event reconstruction and selection criteria used to assign particles to species and energy bin.

The geometrical factor depends on details of the analysis. Especially for the elongated geometry of AMS-02, the inclusion of the ECAL in the required components reduces it significantly. For the compact geometry of calorimetric detectors, this is less important. For high energy electrons and positrons, the geometrical acceptance is of the order of $550\,\mathrm{cm^2 sr}$ for AMS-02 [31], $1200\,\mathrm{cm^2 sr}$ for CALET [25] and $3000\,\mathrm{cm^2 sr}$ for DAMPE [32].

For high-precision results, care must be taken when placing the data points inside their respective bins, especially energy-type variables like kinetic energy (total or per nucleon) or magnetic rigidity on a rapidly falling spectrum. This is often done using the prescription of reference [33]. For high-precision measurements, it is also necessary to account for the bin-to-bin migration of events caused by energy or rigidity resolution. This is usually done by an unfolding procedure.

Three features of generic space detectors are particularly crucial. The first is their ability to establish and monitor the rigidity or energy scale of the measurement. This is important, since an error on the absolute energy or rigidity scale results in an incorrect flux normalisation. To visualise results, one multiplies differential fluxes by a power of the rigidity or energy to make spectral features apparent. The appropriate scale factor is $(\mathrm{d}\Phi/\mathrm{d}R) \cdot R^{2.7}$ for nuclei and $(\mathrm{d}\Phi/\mathrm{d}R) \cdot R^3$ for antiprotons, electrons and positrons. A scale error in rigidity or energy then translates into a shift in the scaled flux.

All modern detectors undergo tests in particle beams at accelerators before flight and the responses of the components measuring the energy or rigidity are calibrated based on these data. However, test beam particles are only available up to few hundred GeV, well below the TeV range. Calorimeters are also calibrated in-flight to correct for time-dependent variation of the energy responses using minimum ionising particles (MIP), which also have low energies. Therefore the check of the energy scale up to TeV requires assumptions on the functional behaviour of the energy response for increasing energy of the incoming particles. Moreover the vibrations and shocks during the launch and the thermal environment in space might change the alignment among the detector layers or the response of the detector. The stability of the rigidity or energy scale is checked in flight by different means:

- In **AMS-02**, the tracker in-flight rigidity scale shift and its uncertainty is obtained comparing the absolute rigidity values measured for electrons and positrons with the energy measured by the electromagnetic calorimeter in 72 energy bins from 2 GeV to 300 GeV [34]. The energy of electrons and positrons is determined with excellent linearity and a resolution of 1.4% at 1 TeV [35,36]. The stability of the rigidity scale as function of time is evaluated analysing the data taken in different time periods and time-dependent corrections are applied. The alignment of the tracker layers is constantly monitored in-flight and corrections are applied. The rigidity scale is thus determined with an accuracy of 3% at 1 TV [20].
- In **CALET**, the detector energy calibration is performed in-flight by checking the consistency of the energy response for proton and helium minimum ionising particles at equivalent rigidity cutoffs. The helium minimum ionising particle peak as a function of the rigidity cutoff, derived from flight data, is compared to Monte Carlo simulations. In addition, the absolute energy scale for nuclei is determined with an accuracy of 3% for protons [37] and 2% of carbon, oxygen, and iron [38,39], based on the precision of the beam test calibration.
- In **DAMPE**, MIP calibration is also performed in-flight. Furthermore, the absolute energy scale uncertainty was estimated using the geomagnetic cutoff for electrons and positrons at 13 GeV, resulting in an accuracy of approximately 1.3% [40,41].

The second important feature concerns the identification of rare species, like positrons or antiprotons. Since their matter counterparts, protons and electrons, are orders of magnitude more abundant, experiments need strong rejection power on the dominant species to determine their flux. So in experiments, light particles like $\mathrm{e^{\pm}}$ must be well separated from heavy particles of like absolute charge, such as protons. In spectrometers, this especially applies to like-sign signal and background, where a rare species must be distinguished from an abundant one. Examples are positrons in a background of protons, antiprotons in a background of electrons. In AMS-02, redundant sub-detectors

are used to increase the background rejection power.

There is a third recurring problem not only for the measurement of elemental spectra but also for their interpretation in terms of cosmic ray propagation. It comes from uncertainties in Monte Carlo simulation. These uncertainties concern the interaction properties of certain cosmic ray species, in particular nuclei. Examples are the energy response of calorimeters or backsplash due to early interactions. The dominant uncertainty, however, comes from our poor knowledge of cross sections for nuclear reactions. Such reactions can transform a heavier element into a lighter one by inelastic interaction. The target can be interstellar matter, mostly protons and helium nuclei, met before the cosmic ray reaches us. The transformation probability must then be taken into account in modelling spectra and composition of cosmic rays. The extraction of propagation parameters strongly relies on the knowledge of spallation cross sections. The identification of signals from dark matter or primordial antimatter requires a precise determination of the background from secondary production of positrons, antiprotons and anti-nuclei. If one could firmly establish the probability for secondary production, this would serve as benchmark to identify excesses or deficits in observed cosmic ray spectra and pin down their origin, acceleration mechanism and propagation history.

The target for nuclear reactions can also be met inside the detector itself, the loss and gain in the initial and final species must then be corrected for. The poor knowledge of nuclear fragmentation cross sections thus affects also cosmic ray measurements themselves and contributes a sizeable systematic error. In particular, the knowledge of the amount of incoming cosmic ray nuclei fragmenting in the detector material is of paramount importance to correctly assess the overall flux normalisation. There are two principle approaches to this problem. One can estimate the survival probability of a given nucleus using simulation. The systematic error is then estimated comparing different nuclear interaction models or comparing Monte Carlo simulations to test beam data [41]. An alternative and more robust approach is to compare the simulation to data collected with the detector itself [20, 38, 42]. At energies below a few hundred GeV/n, this can be done using test beam data. At high energy, cosmic ray data can be used to measure survival probabilities in the detector, provided the detector design allows to clearly identify incoming nuclei before they start to fragment, to use a portion of the detector as target, and to measure the amount of fragmentation products on the downstream side. With this approach, the AMS-02 detector has measured charge-changing nuclear fragmentation cross sections on carbon target for the most abundant primary cosmic ray nuclei from helium to iron with rigidities from few GV up to TV [43, 44]. DAMPE has made a similar study for protons and helium nuclei impinging on heavy target material [45].

4. Conclusions and Outlook

Cosmic ray experiments with sophisticated hardware inherited from accelerator-based particle physics are currently operating in space. They provide crucial information on the spectra and composition of cosmic rays near Earth. Measurements of rare components also contribute to the search for new particles. Current experiments cover an energy range up to PeV for protons and nuclei, several TeV for electrons and positrons. Calorimetric detectors like CALET and DAMPE concentrate on reaching the highest possible energies, identifying leptons and nuclear species. The spectrometric detector AMS-02 provides separation between particles and antiparticles and isotopes at the expense of a somewhat reduced energy reach. The long term exposure and carefully maintained performance of the detectors allow an ever increasing detail of the measurements and unprecedented statistical accuracy. Methodology proven in ground-based experiments ensures proper control of systematics.

While maintenance and upgrades of detectors on free-flying satellites are the absolute exception, the ISS provides a platform where the threshold for human intervention is lower, although non-negligble. An example is the replacement of the thermal control system for AMS-02 in 2019 [46] (See https://ams02.space/upgraded-tracker-thermal-pump-system (accessed on 24 September 2025)). In the near future, a further layer of silicon microstrip detectors will be added on the very top of AMS-02 [47]. This will increase the geometrical acceptance by a factor 3 for many analyses. It will also improve the measurement of the absolute particle charge due to the low material budget in front of the new detector.

Direct detection of cosmic rays in space will see future projects following the two basic approaches: calorimetric measurements and magnetic spectroscopy. Probably the next observatory in line will be the High Energy Radiation Detector (HERD) [48–50] of the Chinese Space Agency. The detector will be accommodated on the Chinese Space Station CSS, which is currently under construction. The core of the detector is a novel calorimeter made of small cubic elements with three-dimensional read-out, inspired by the CaloCube project [51]. It will allow to not only accept cosmic rays entering through the zenith face but also through the lateral faces, thus greatly increasing the accepted solid angle. Despite its compact size of less than a m^3 and a weight of less than $4\,\mathrm{t}$, the acceptance of HERD will reach several $\mathrm{m}^2\,\mathrm{sr}$. The fine segmentation, highly sensitive material and unprecedented depth of the calorimeter will allow to reliably separate $\mathrm{e}^{\pm}$ from nuclei up to $100\,\mathrm{TeV}$ and measure their energy with

percent resolution. Large acceptance and long term exposure on the space station will enable identification and energy measurement of nuclei beyond PeV energies.

In a more distant future, two projects for follow-up spectrometers aim at acceptances extended by an order of magnitude. Two design studies [52,53] have been submitted to the ESA program "Voyage 2050", called AMS-100 [54] and ALADInO [55], respectively. Both intend to surround a 3D calorimeter inspired by the HERD design with a magnetic spectrometer. To avoid having to cool their magnet coils to superconducting temperatures, they will use warm superconductors at a few tens of Kelvin, in thermal equilibrium with the local environment if sunshine is efficiently shielded. Both detectors are intended to operate at Lagrange point 2, about $1.5 \times 10^9\,\mathrm{km}$ away from Earth, where the combined gravitational fields of Sun and Earth are in equilibrium with the centrifugal force on a co-rotating object.

Funding

The research received no external funding.

Conflicts of Interest

The author declares no conflict of interest.

Use of AI and AI-Assisted Technologies

No AI tools were used for this paper.

References

1. Van Allen, J.A.; Tatel, H.E. The cosmic-ray counting rate of a single Geiger counter from ground level to 161 kilometers altitude. *Phys. Rev.* **1948**, *73*, 245–251.
2. Grigorov, N.L.; Nesterov, V.E.; Rapoport, I.D.; et al. Investigation of Energy Spectrum of Primary Cosmic Particles with High and Super-High Energies of Space Station PROTON. *Yad. Fiz.* **1970**, *11*, 1058–1069.
3. Grigorov, N.L.; Mamontova, N.A.; Rapoport, I.D.; et al. Energy Spectrum of Primary Cosmic Rays in the 10^{11}–10^{15}eV Energy Range According to the Data of Proton-4 Measurements. In Proceedings of the 12th International Cosmic Ray Conference, Hobart, TAS, Australia, 16–25 August 1971; Volume 5, pp. 1746–1751.
4. Grigorov, N.L.; Mamontova, N.A.; Rapoport, I.D.; et al. On Irregularity in the Primary Cosmic Ray Spectrum in the 10^{12} eV Energy Range. In Proceedings of the 12th International Cosmic Ray Conference, Hobart, TAS, Australia, 16–25 August 1971; Volume 5, pp. 1752–1759.
5. Grigorov, N.L.; Rapoport, I.D.; Savenko, I.A.; et al. Energy Spectrum of Cosmic Ray α-Particles in 5×10^{10}–10^{12} eV/Nucleon Energy Range. In Proceedings of the 12th International Cosmic Ray Conference, Hobart, TAS, Australia, 16–25 August 1971; Volume 5, pp. 1760–1768.
6. Grigorov, N.L.; Tolstaya, E.D. The spectrum of cosmic-ray particles and their origin. *JETP* **2004**, *98*, 643–650.
7. Grigorov, N.L.; Rapoport, I.D.; Savenko, I.A.; et al. Some problems and perspectives in cosmic-ray studies. *Space Sci. Rev.* **1966**, *5*, 167–209.
8. Ivanenko, I.P.; Rapoport, I.D.; Shestoperov, V.Y.; et al. Energy spectrum of primary cosmic-ray particles at 1–100 TeV from data from the Sokol package. *JETP Lett.* **1989**, *49*, 222–224.
9. Atkin, E.; Bulatov, V.; Dorokhov, V.; et al. The NUCLEON space experiment for direct high energy cosmic rays investigation in TeV–PeV energy range. *Nucl. Instrum. Meth. A* **2015**, *770*, 189–196.
10. Spillantini, P. CR from Space Based Observatories: History, Results and Perspectives of the PAMELA Mission. In Proceedings of the 9th Baikal Summer School on Physics of Elementary Particles and Astrophysics, Bol'shie Koty, Russia, 23–30 July 2009; pp. 213–234.
11. Adriani, O.; Bonechi, L.; Bongi, M.; et al. The Magnetic Spectrometer of the PAMELA Experiment: On-Ground Test of the Flight-Model. In Proceedings of the 20th ICRC, Pune, Pune, India, 3–10 August 2005; Volume 3, pp. 317–320.
12. Pamela Collaboration, Adriani, O.; Barbarino, G.C.; et al. Ten years of PAMELA in space. *Riv. Nuovo Cim.* **2017**, *40*, 473–522.
13. Adriani, O.; Barbarino, G.C.; Bazilevskaya, G.A.; et al. An anomalous positron abundance in cosmic rays with energies 1.5–100 GeV. *Nature* **2009**, *458*, 607–609.
14. Adriani, O.; Barbarino, G.C.; Bazilevskaya, G.A.; et al. Cosmic-ray positron energy spectrum measured by PAMELA. *Phys. Rev. Lett.* **2013**, *111*, 081102.
15. Bonechi, L.; Adriani, O.; Bongi, M.; et al. Status of the PAMELA silicon tracker. *Nucl. Instrum. Meth. A* **2007**, *570*, 281–285.
16. Bindi, V.; Paniccia, M.; Pohl, M. *Cosmic Ray Physics: An Introduction to the Cosmic Laboratory*; CRC Press: Boca Raton, 2023.

17. Aguilar, M.; Alcaraz, J.; Allaby, J.; et al. The Alpha Magnetic Spectrometer (AMS) on the International Space Station: Part I—results from the test flight on the space shuttle. *Phys. Rep.* **2002**, *366*, 331–405.
18. Yamamoto, A.; Mitchell, J.W.; Yoshimura, K.; et al. Search for cosmic-ray antiproton origins and for cosmological antimatter with BESS. *Adv. Space Res.* **2013**, *51*, 227–233.
19. Abe, K.; Fuke, H.; Haino, S.; et al. The results from BESS-Polar experiment. *Adv. Space Res.* **2017**, *60*, 806–814.
20. Aguilar, M.; Cavasonza, L.A.; Ambrosi, G.; et al. The Alpha Magnetic Spectrometer (AMS) on the International Space Station: Part II – Results from the first seven years. *Phys. Rep.* **2021**, *894*, 1–116.
21. Chang, J.; Ambrosi, G.; An Q.; et al. The DArk Matter Particle Explorer mission. *Astrop. Phys.* **2017**, *95*, 6–24.
22. Torii, S.; Marrocchesi, P.S. The CALorimetric Electron Telescope (CALET) on the International Space Station. *Adv. Space Res.* **2019**, *64*, 2531–2537.
23. Asaoka, Y.; Adriani, O.; Akaike, Y.; et al. The CALorimetric Electron Telescope (CALET) on the International Space Station: Results from the first two years on orbit. *J. Phys.: Conf. Ser.* **2019**, *1181*, 012003.
24. Asaoka, Y.; Akaike, Y.; Komiya, Y.; et al. Energy calibration of CALET onboard the International Space Station. *Astropart. Phys.* **2017**, *91*, 1–10.
25. Adriani, O.; Akaike, Y.; Asano, K.; et al. Direct Measurement of the Spectral Structure of Cosmic-Ray $\mathrm{Electrons} + \mathrm{Positrons}$ in the TeV Region with CALET on the International Space Station. *Phys. Rev. Lett.* **2023**, *131*, 191001.
26. Seo, E.S.; Anderson, T.; Angelaszek, D.; et al. Cosmic Ray Energetics And Mass for the International Space Station (ISS-CREAM). *Adv. Space Res.* **2014**, *53*, 1451–1455.
27. Seo, E.S.; Amare, Y.; Angelaszek, D. Cosmic Ray Energetics And Mass for the International Space Station (ISS-CREAM). In Proceedings of the 36th International Cosmic Ray Conference—ICRC2019, Madison, WI, USA, 24 July–1 August 2019.
28. Choi, G.H.; Seo, E.S.; Aggarwal, S.; et al. Measurement of High-Energy Cosmic-Ray Proton Spectrum from the ISS-CREAM Experiment. *Astrophys. J.* **2022**, *940*, 107.
29. Sun, H.; Alemanno, F.; Altomare, C.; et al. Measurement of Heavy Nuclei Beyond Iron in Cosmic Rays with the DAMPE Experiment. In Proceedings of the 38th International Cosmic Ray Conference, Nagoya, Japan, 26 July–3 August 2023.
30. Alemanno, F.; Altomare, C.; An Q.; et al. Measurement of the cosmic $p + \mathrm{He}$ energy spectrum from 50 GeV to 0.5 PeV with the DAMPE space mission. *Phys. Rev. D* **2024**, *109*, L121101.
31. Aguilar, M.; Aisa, D.; Alvino, A.; et al. Electron and Positron Fluxes in Primary Cosmic Rays Measured with the Alpha Magnetic Spectrometer on the International Space Station. *Phys. Rev. Lett.* **2014**, *113*, 121102.
32. Fan, R.R.; Zhang, F.; Peng, W.X.; et al. The silicon matrix for the prototype for the Dark Matter Particle Explorer. *arXiv* **2024**, arXiv:physics.ins-det/1403.1679.
33. Lafferty, G.D.; Wyatt, T.R. Where to stick your data points: The treatment of measurements within wide bins. *Nucl. Instrum. Meth. A* **1995**, *355*, 541–547.
34. Berdugo, J.; Choutko, V.; Delgado, C.; et al. Determination of the rigidity scale of the Alpha Magnetic Spectrometer. *Nucl. Instrum. Meth. A* **2017**, *869*, 10–14.
35. Adloff, C.; Basara, L.; Bigongiari, G.; et al. The AMS-02 lead-scintillating fibres electromagnetic calorimeter. *Nucl. Instrum. Meth. A* **2013**, *714*, 147–154.
36. Kounine, A.; Weng, Z.; Xu, W.; et al. Precision measurement of $0.5\ \mathrm{GeV}$–$3\ \mathrm{TeV}$ electrons and positrons using the AMS electromagnetic calorimeter. *Nucl. Instrum. Meth. A* **2017**, *869*, 110–117.
37. Adriani, O.; Akaike, Y.; Asano, K.; et al. Direct measurement of the cosmic-ray proton spectrum from 50 GeV to 10 TeV with the Calorimetric Electron Telescope on the International Space Station. *Phys. Rev. Lett.* **2019**, *122*, 181102.
38. Adriani, O.; Akaike, Y.; Asano, K.; et al. Direct measurement of the cosmic-ray carbon and oxygen spectra from 10 GeV/*n* to 2.2 TeV/*n* with the Calorimetric Electron Telescope on the International Space Station. *Phys. Rev. Lett.* **2020**, *125*, 251102.
39. Adriani, O.; Akaike, Y.; Asano, K.; et al. Measurement of the iron spectrum in cosmic rays from $10\ \mathrm{GeV}/n$ to $2.0\ \mathrm{TeV}/n$ with the Calorimetric Electron Telescope on the International Space Station. *Phys. Rev. Lett.* **2021**, *126*, 241101.
40. Zang, J.; Yue, C.; Li, X. Measurement of Absolute Energy Scale of ECAL of DAMPE with Geomagnetic Rigidity Cutoff. In Proceedings of the 35th International Cosmic Ray Conference—ICRC2017, Bexco, Korea, 10–20 July 2017.
41. Alemanno, F.; An Q.; Azzarello, P.; et al. Measurement of the cosmic ray helium spectrum from 70 GeV to 80 TeV with the DAMPE space mission. *Phys. Rev. Lett.* **2021**, *126*, 201102.
42. Aguilar, M.; Aisa, D.; Alpat, B.; et al. Precision Measurement of the helium flux in primary cosmic rays of rigidities 1.9 GV to 3 TV with the Alpha Magnetic Spectrometer on the International Space Station. *Phys. Rev. Lett.* **2015**, *115*, 211101.
43. Yan, Q.; Choutko, V.; Oliva, A.; et al. Measurements of nuclear interaction cross sections with the Alpha Magnetic Spectrometer on the International Space Station. *Nucl. Phys. A* **2020**, *996*, 121712.
44. Aguilar, M.; Cavasonza, L.A.; Allen, M.S.; et al. Properties of Iron primary cosmic rays: Results from the Alpha Magnetic Spectrometer. *Phys. Rev. Lett.* **2021**, *126*, 0411104.
45. Alemanno, F.; An Q.; Azzarello, P.; et al. Hadronic cross section measurements with the DAMPE space mission using 20 GeV–10 TeV cosmic-ray protons and ^{4}He. *Phys. Rev. D* **2025**, *111*, 012002.
46. van Es, J.; Pauw, A.; van Donk, G.; et al. AMS02 Tracker Thermal Control Cooling System Commissioning and Operational Results. In Proceedings of the 43rd International Conference on Environmental Systems, Vail, CO, USA, 14–18 July 2013.

47. Ambrosi, G. The Silicon Tracker L0 Upgrade of the AMS-02 experiment on the ISS. In Proceedings of the Advances in Space AstroParticle Physics (ASAPP 2025), Lisbon, Portugal, 12–16 May 2025.
48. Zhang, S.N.; Adriani, O.; Albergo, S.; et al. The High Energy Cosmic-Radiation Detection (HERD) Facility Onboard China's Space Station. In *Space Telescopes and Instrumentation 2014: Ultraviolet to Gamma Ray, Proceedings of the SPIE Astronomical Telescopes + Instrumentation Conference, Montreal, QC, Canada, 22–26 June 2014*; Takahashi, T., den Herder, J.-W.A., Bautz, M., Eds.; SPIE: Bellingham, WA, USA, 2014; Volume 9144, pp. 293–301.
49. Kyratzis, D.; HERD collaboration. Overview of the HERD space mission. *Phys. Scr.* **2022**, *97*, 054010.
50. Cagnoli, I.; Kyratzis, D.; Serini, D.. HERD space mission: Probing the Galactic Cosmic Ray frontier. *Nucl. Instrum. Meth. A* **2024**, *1068*, 169788.
51. Adriani, O.; Albergo, S.; Auditore, L.; et al. The CALOCUBE project for a space based cosmic ray experiment: design, construction, and first performance of a high granularity calorimeter prototype. *J. Inst.* **2019**, *14*, P11004.
52. Schae, S.; Atanasyan, A.; Berdugo, J.; et al. AMS-100: The next generation magnetic spectrometer in space—An international science platform for physics and astrophysics at Lagrange point 2. *Nucl. Instrum. Meth. A* **2019**, *944*, 162561.
53. Battiston, R.; Bertucci, B.; Adriani, O.; et al. High precision particle astrophysics as a new window on the universe with an Antimatter Large Acceptance Detector In Orbit (ALADInO). *Exper. Astron.* **2021**, *51*, 1299–1330.
54. Chung, C.; Backes, T.; Dittmar, C.; et al. The development of SiPM-based fast time-of-flight detector for the AMS-100 experiment in space. *Instruments* **2022**, *6*, 14.
55. Adriani, O.; Altomare, C.; Ambrosi, G.; et al. Design of an Antimatter Large Acceptance Detector In Orbit (ALADInO). *Instruments* **2022**, *6*, 19.